

Taming Chaos: Stabilization of Aperiodic Attractors by Noise

Walter J. Freeman, H.-J. Chang, B. C. Burke, P. A. Rose, and J. Badler

Abstract—A model named “KIII” of the olfactory system contains an array of 64 coupled oscillators simulating the olfactory bulb (OB), with negative and positive feedback through low-pass filter lines from single oscillators simulating the anterior olfactory nucleus (AON) and prepyriform cortex (PC). It is implemented in C to run on Macintosh, IBM, or UNIX platforms. The output can be set by parameter optimization to point, limit cycle, quasi-periodic, or aperiodic (presumably chaotic) attractors. The first three classes of solutions are stable under variations of parameters and perturbations by input, but they are biologically unrealistic. Chaotic solutions simulate the properties of time-dependent densities of olfactory action potentials and EEG’s, but they transit into the basins of point, limit cycle, or quasi-periodic attractors after only a few seconds of simulated run time. Despite use of double precision arithmetic giving 64-bit words, the KIII model is exquisitely sensitive to changes in the terminal bit of parameters and inputs. The global stability decreases as the number of coupled oscillators in the OB is increased, indicating that attractor crowding reduces the size of basins in the model to the size of the digitizing step ($\sim 10^{-16}$). Chaotic solutions having biological verisimilitude are robustly stabilized by introducing low-level, additive noise from a random number generator at two biologically determined points: rectified, spatially incoherent noise on each receptor input line, and spatially coherent noise to the AON, a global control point receiving centrifugal inputs from various parts of the forebrain. Methods are presented for evaluating global stability in the high dimensional system from measurements of multiple chaotic outputs. Ranges of stability are shown for variations of connection weights (gains) in the KIII model. The system is devised for pattern classification.

Index Terms—Additive noise, attractor crowding, chaos, electroencephalography, neural network, olfactory system, pattern classification, stability assay.

I. INTRODUCTION

EXPERIMENTS in animals reveal that the electroencephalograms (EEG’s) of the primary sensory cortices for vision, audition, olfaction, and touch have spatiotemporal patterns relating to external stimuli [1], [2]. The patterns have the form of spatial amplitude modulation of a broad spectrum, aperiodic wave form [3], that is common to all the 8×8 traces simultaneously recorded at the cortical surfaces. Following training of the experimental subjects to respond to conditioned stimuli, the spatial patterns, expressed as 64×1 column vectors, can be classified in respect to the discriminated conditioned stimuli. In the language of dynamics, each sensory cortex maintains a low dimensional

global aperiodic attractor with multiple “wings,” one for each class of learned stimuli [4]. During an act of perception the activity of the cortex is confined into an appropriate “wing” by which the appropriate spatial pattern occurs. The process can be modeled by a stimulus-induced state transition in a complex dynamical system, which is composed of an array of coupled nonlinear oscillators based in excitatory and inhibitory neuron ensembles, and which maintains a stable chaotic state before and after step inputs are given. The long-range purpose is to use nonlinear dynamics in fast and accurate pattern recognition in simulation of the capabilities of biological intelligence [5], [6]. The present aim is to evaluate the stability of the extant model.

The KIII model of the olfactory system consists of a set of parametric ordinary differential equations [7], which become difference equations (ODE’s) in a digital embodiment [8]–[10]. They incorporate the synaptic connections and express the physiological time delays and distributed interactions among the cell ensembles. The model has an unspecified number of point, limit cycle, quasi-periodic, and chaotic attractors [11]. Examination of solutions in the first three classes has shown them to be stable under perturbation by inputs and variation of parameter values on the order of 5–50% of center values, optimized by methods previously described [12].

However, the high-dimensional ODE set parameterized to give chaotic behavior reveals an exquisite sensitivity to any small change in input or in a parameter value, which is revealed by loss of a previously optimized aperiodic trajectory. Further, when free running in a chaotic mode, sooner or later the model undergoes a state transition from an assigned chaotic attractor to a new stable orbit or point. A measure of this instability is the time from initialization to the onset of the transition [13]. Stability decreases with increasing size of the array of coupled oscillators. An exceedingly small numerical perturbation in parameters or variables can change the state of the whole system from one attractor to another, indicating that it is due to attractor crowding [14]–[16], by which the size of the basins shrinks to the scale of the word size in double precision arithmetic that gives a digital increment of 1 in 64 bits.

Prior studies of chaotic systems have emphasized the suppression of chaos or the entrainment of two or more elements into the same aperiodic time series. In the present study the effects were studied of additive noise on the stability of chaotic attractors in an extension of preliminary work [13]. Prior work to control chaos has been focused on suppressing chaos or phase locking chaotic generators [17], [18]. Most prior uses

Manuscript received January 28, 1997; revised June 16, 1997. This work was supported by the Office of Naval Research Grant N00014-90-J-4054. This paper was recommended by Guest Editor M. J. Ogorzałek.

The authors are with the Division of Neurobiology, University of California, Berkeley, CA 94720 USA.

Publisher Item Identifier S 1057-7122(97)07317-0.

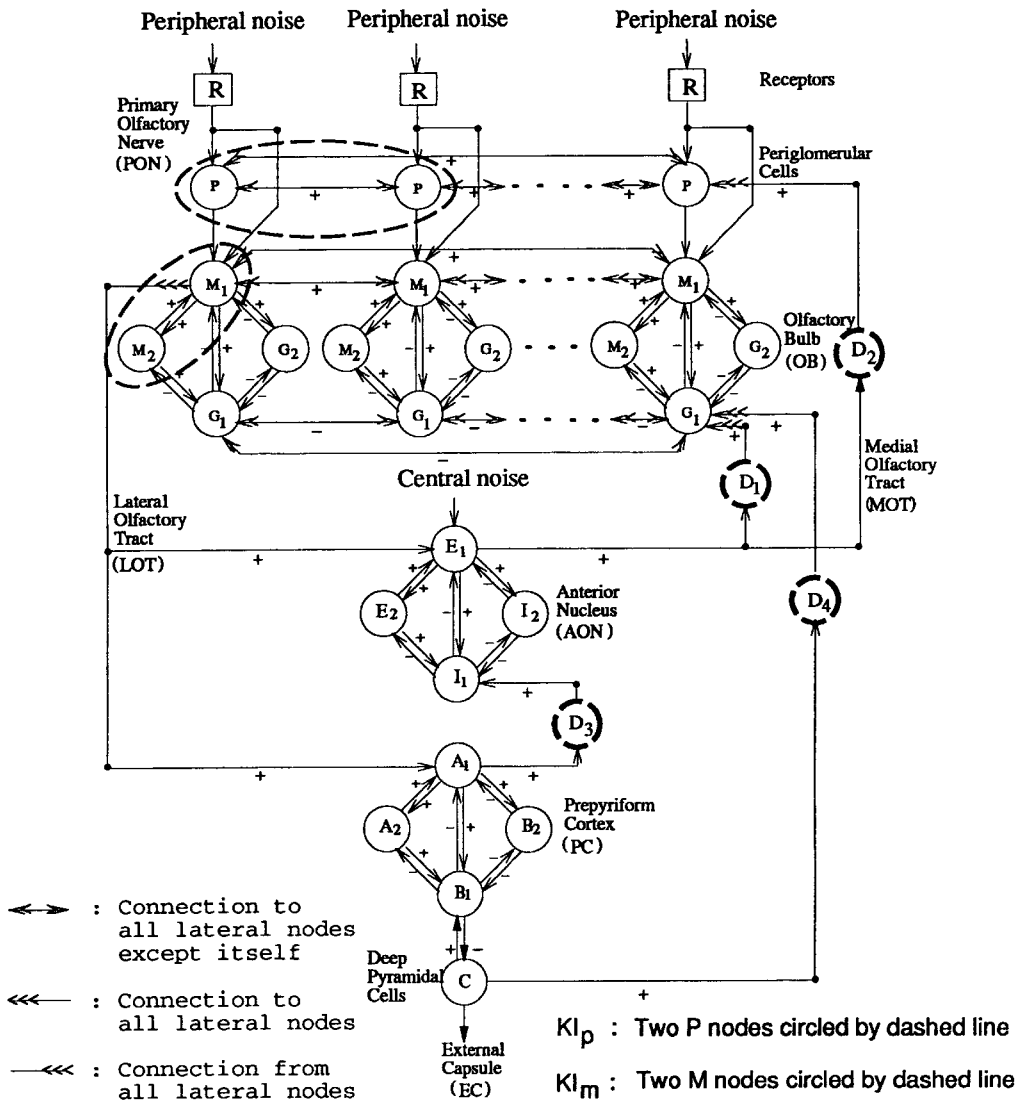


Fig. 1. The topologic diagram of the olfactory system is based in the anatomical and physiological properties. Noise from external sources is given at the receptors. Central noise is focused into the anterior olfactory nucleus (KII_{aon}).

of noise have been to achieve destabilization, as in simulated annealing and stochastic resonance [19]. Liljenström and Wu [20] found that activity expressed as temporal noise in an associative neural network reduced recall time in associative memory tasks. Billah and Shinozuka [21] reported stabilization of nonlinear networks by multiplicative noise. Wackerbauer [22] used noise to stabilize the Lorenz attractor. Fryska and Zohdy [23] put a Markovian process on every ordinary differential equation (ODE) of a three-dimensional piecewise linear system to randomize the rounding-off of floating point arithmetic in numerical simulation. They used the shadowing lemma to assure the existence of a numerically shadowed trajectory. Since each point on a digital trajectory is merely close to a corresponding point of the true trajectory, the computed trajectory is shadowed by the true trajectory [24], [25]. Because the olfactory system and its KIII model both have Lyapunov exponents for which the real parts fluctuate above and below zero [7], the KIII model cannot solve the shadowing problem, owing to the resulting numerical instabilities [12], [13], [16], [25].

In Section II the KIII model is briefly reviewed, and the types of noise are described along with the nodes of injection and the reasons for choosing those nodes. The state variables and the equations have already been described in detail [5], [6], [8], [12]. In Section III the criteria are listed and described, according to which the aperiodic outputs of nodes in the KIII model are optimized to conform to biological measurements, and some representative traces, power spectra, and amplitude histograms are shown. In Section IV algorithms are given to evaluate the global stability of the KIII model in aperiodic states. The ranges are shown for the variations of input and of the important parameters over which stability obtains. Results are discussed and evaluated in Section V.

II. THE HYBRID KIII MODEL WITH ADDITIVE NOISE

A. KIII Topology

The central olfactory system consists of the bulb (OB), anterior olfactory nucleus (AON), and prepyriform cortex

(PC). Input from receptors (R) goes to periglomerular (P), and mitral cells (M). The mitral cells transmit to granule cells (G) and to AON and PC, from which the final output is sent to the external capsule (EC) from deep pyramidal cells (C), as well as back to the OB and AON. The nodes in the topological diagram (Fig. 1) represent neural aggregates. When the neurons in an aggregate have no interactions with others, they are represented by a KO set, as for example R and C . An aggregate of interactive neurons is represented by a KI set, consisting of a transmitting KO set and a receiving KO set undergoing continuous renewal. Mutually excitatory neurons form a KI_e set (P , M , E , and A), and mutually inhibitory neurons form a KI_i set (G , I , and B), both comprising positive feedback and having only zero and nonzero point attractors. The interaction of excitatory and inhibitory neuron populations forms a KII set (OB, AON, and PC), which has point, limit cycle, and quasi-periodic attractors. The interaction of the KI_p set and the three KII sets is modeled with the KIII set. Feedforward transmission through the lateral olfactory tract is fast, so delays are not explicitly introduced. Feedback through the medial olfactory tract (MOT) is slow and dispersed, owing to the distributions of axonal conduction velocities and distances [7]. Delays are modeled by second order low-pass filters [12].

The excitatory and inhibitory neurons in the OB, AON, and PC form sheets of neuropil without discrete internal boundaries in directions parallel to the surface of the brain. R input axons are spatially coarse-grained by glia forming glomeruli, which are nests of axons, dendrites and their synapses. The KII_{ob} set is represented by an 8×8 array of KII subsets, that are fully interconnected at the M_1 and G_1 nodes, conforming to a toroidal boundary condition. The KII_{aon} and KII_{pc} sets are in lumped form in the present stage of development of the KIII model.

In digital embodiments the dynamics is re-formulated from ODE's into difference equations. The continuous tissue is represented in the model by as many spatial compartments for the KI and KII subsets as computational resources can support. Continuous time is replaced with discrete time steps. Numerical solutions to the ODE's were obtained with the Livermore Solver (LSODE) [12]. The basic time step was set at 1 ms and was flexibly adjusted to shorter lengths, depending on the local rate of change of the state variable under integration.

B. State Variables and Reciprocal Conversions

The dynamics of each node is represented by a linear second order ODE with two real rate constants, which are evaluated from the rates of rise and decay of OB, AON, and PC impulse responses in the open loop state established under deep anesthesia. State variables are continuous in time in the wave mode v corresponding to EEG measurements of dendritic current density, and in the pulse mode p corresponding to extracellular observations of action potentials, and to the outputs of the OB, AON, and PC to each other and other parts of the brain. The synapses convert axonal pulse density to dendritic wave density. The synaptic weights at the inputs

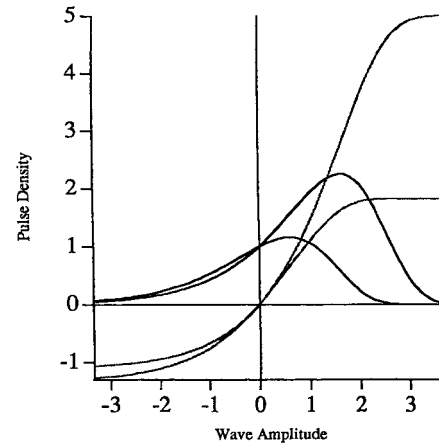


Fig. 2. The sigmoid curve, shown for two values of $Q_m = 1.82$ and 5.0 , shows pulse density, q , as a function of wave density, v , where Q_m is the upper asymptote of q . The derivative of the function, dq/dv , gives the nonlinear gain. The peak gain is at the value v_{max} . $q = Q_m \{1 - \exp[-(e^v - 1)/Q_m]\}$, $dp/dv = \exp[v - (e^v - 1)/Q_m]$, $v_{max} = \ln(Q_m)$.

of axons to dendrites are represented by gain coefficients, k_{ij} from the j th to the i th node. Trigger zones at cell bodies convert dendritic current density to pulse density. In neural populations the wave-pulse conversion is given by a static nonlinear function, the asymmetric sigmoid curve (Fig. 2), with a single parameter Q_m that determines the maximal pulse density, the mean firing density, and the steepness of the curve. The derivative gives the nonlinear gain dp/dv [4], [8], that has its maximal value at wave amplitude $v_{max} = \ln(Q_m)$.

The range of wave-pulse conversion holds the pulse-wave conversion at synapses within a small-signal, near-linear range, which makes it possible to represent it by a gain coefficient. It is the nonlinearity at the trigger zones that mediates the stability of the KIII set and its components. The KI_p set has a nonzero point attractor that maintains its operation above the wave value of maximal slope of the sigmoid, so that excitatory input decreases its loop gain, and inhibitory input increases it [8], [27]. The KI_m set is stabilized at a point or limit cycle attractor that keeps its operation below the value of maximal slope. Inhibitory input stabilizes it by reducing its loop gain, and excitatory input increases its loop gains. For high values of $Q_m \geq 5$, which occur in animals that are motivated to search for odors, R input destabilizes the basal state. The entire OB transits to near-periodic oscillation in the gamma range (g , $40 < f < 100$ Hz) on inhalation, and it returns to the basal state during exhalation, during which the R are not activated.

The asymmetry of the nonlinear conversion of wave to pulse density at trigger zones is essential for the mechanism of input-dependent state transitions from the background, $1/f$ -type state to the narrow-band oscillation in the burst state. The transition is facilitated by increase in the KI_m gains between selected subsets of excitatory neurons, during learning in accordance with the Hebb rule, which shapes a matrix of coefficients resembling those in Amari, Hopfield, Anderson, and Kohonen associational networks. The state transition is blocked by reduction of the gains of selected K_{m1}

nodes to other KII_{ob} nodes. This occurs during habituation to insignificant or ambiguous or background odors during learning. The reduction enhances oscillatory responses to repetitive input in the delta range (d , $1 < f < 10$ Hz), which includes the respiratory driving frequencies, so that habituation to background inputs facilitates the destabilization to foreground odor input [4], [8], because the habituated input augments the nonspecific excitatory bias of background input. The gamma/delta (g/d) ratio in the power spectrum of KIII aperiodic time series offers a useful criterion of system performance.

C. Inputs of Stimuli and Noise

A small impulse to one or more of the R nodes serves to initiate activity, starting from an unstable zero point and transiting to a basal aperiodic attractor of the KIII model. Simulated sensory input given to multiple R nodes is normalized to give a fixed total amplitude, that is optimized and compressed on the scale of a power function. This operation is derived from and comparable to the normalization and dynamic range compression that is performed on olfactory receptor input into the OB [7] by the periglomerular cells (KI_p). Input from R nodes in the pulse density mode is discretized in time at 1 ms intervals and in space to the KI_{p_1} and KI_{m_1} subsets. The wave form of the simulated sensory input is a 200 ms step function with the leading and trailing edges rounded by a half cycle of a 50 Hz cosine with its mean amplitude set at half the amplitude of the step. This form models the respiratory cycle, and it reduces the ringing in the model that is observed with impulse inputs [8]. Noise is made with a random number generator giving a normal density function with zero mean and unit standard deviation (SD). The noise is added at two locations, corresponding to the two sources of external perturbation of the olfactory system [27]. Input by way of the receptor axons is purely excitatory, and their firings are locally uncorrelated. The Gaussian noise is full-wave rectified, and an independent time series is added to each R line to the KI_{p_1} and KI_{m_1} nodes. Centrifugal inputs from various parts of the brain to the olfactory system are concentrated into the AON, which serves as a subsidiary control center. Its output is broadly distributed to the OB by its divergent feedback projection. The inputs are predominantly excitatory, so random number time series is off-set by +1 SD. It is added to the LOT input to KI_{e_1} node, from which it is disseminated as spatially coherent noise. It is smoothed by the low-pass filters in the MOT delay lines. The amplitudes of the two noise SD's are optimized as described below. The input and output of the KI_{e_1} node are not significantly correlated, showing that the noise is not simply amplified and fed back into the system.

III. SIMULATION OF EEG'S AND PULSE DENSITIES

A. Criteria for Optimization of Performance

Parameter optimization algorithms are used to determine the parameter values required to simulate the experimental data from measurements of the EEG and action potentials from the

neural populations of the olfactory system. The criteria for optimization are that the KIII outputs have

- 1) stable and robust aperiodic oscillations having near $1/f$ -type power spectra;
- 2) nearly periodic oscillations with peaks in the gamma g range during excitatory inputs corresponding to EEG bursts on inhalation;
- 3) spatially coherent wave forms over all subsets of the KI_{m_1} nodes and also of the KI_{g_1} nodes in the KII_{ob} , both in and between bursts;
- 4) transition from background to burst in <10 ms with the stated input;
- 5) amplitude histograms in both wave and pulse modes that are nearly Gaussian;
- 6) means and distributions of periglomerular cell KI_p outputs above the point of maximal slope of the sigmoid and below the maximal (excitatory) asymptote;
- 7) means and distributions of mitral KI_m and granule KI_g outputs below the point of maximal slope of the sigmoid and above the minimal asymptote;
- 8) nearly equal means for the KI_{g_1} and KI_{g_2} nodes;
- 9) and nearly zero offset of the means for the mitral cell KI_m nodes, irrespective of the mean amplitudes of the KI_{g_1} and KI_{g_2} nodes.

Representative parameter values keyed to Fig. 1 are listed in Table I. These are useful starting guesses for optimization of the KIII model on any other platform, but cannot be expected to reproduce on other platforms precisely the chaotic time series illustrated here.

B. An Assay of Sensitivity for Destabilization

As optimization of parameters to achieve these criteria proceeded, the KIII system without noise became progressively less stable and more likely to transit to a point or limit cycle attractor spontaneously. An assay of sensitivity was discovered following a routine change in programming. A line of code calling for repeated division by a constant was changed to repeated multiplication by the reciprocal. Though mathematically equivalent, one version transited to sustained aperiodic oscillation, whereas the other gave a quasi-periodic oscillation after <1 s of simulated run time. This change implicated the round-off error in the terminal bit. Zak [28] used randomization of the terminal bits in digital state variables to simulate neurodynamics with "terminal chaos." In the absence of a shadow trajectory, one version was used to track the other one, and the sensitivity was measured by the run time to detect divergence of the two versions ([13, Figs. 12 and 13]). By this test the randomization of the terminal bit in all of the state variables was found to delay but not prevent divergence of the two time series or eventual transition from an aperiodic orbit to a point or limit cycle attractor. Furthermore, any minute change in the input amplitude or in any parameter so changed the global performance of the KIII system, that the parameter set had to be re-optimized to bring the KIII output within the above criteria.

The addition of the designated noise stabilized the system, both in respect to changes of input and of parameters. An

TABLE I
GIVEN THE SPECIFIED INPUT WAVE FORM, THE LINEAR RATES
AND DELAYS, AND THE NONLINEAR SIGMOID FUNCTIONS,
THERE WERE 24 GAIN PARAMETERS TO BE OPTIMIZED

Parameter:	initial value	minimal	maximal
For n-channel KI_p :			
k_{pr}	0.500	0.008	1.100
k_{pp}	0.900	0.900	1.300
For n-channel KI_{Ob} :			
k_{mm}	1.600	0.350	2.400
k_{gm}	1.723	1.400	2.400
k_{mg}	2.363	2.000	2.900
k_{gg}	2.245	1.900	2.400
k_{m1r}	1.000	0.008	3.000
k_{m1p}	0.050	0.002	0.760
For KI_{aon} :			
k_{ee}	1.200	0.390	1.202
k_{ie}	1.372	0.930	2.100
k_{ei}	1.426	0.790	2.300
k_{ji}	1.571	0.760	1.700
For KI_{pc} :			
k_{ga}	0.823	0.006	1.200
k_{ba}	1.947	0.790	2.300
k_{ab}	1.938	0.900	2.500
k_{bb}	2.354	2.300	3.200
k_{bc}	0.698	0.498	2.098
k_{cb1}	1.543	1.044	4.544
For MOT gains:			
k_{g1d1}	2.349	1.649	3.349
k_{pd2}	1.087	0.287	3.587
k_{i1d3}	2.553	0.003	9.553
k_{g1d4}	2.305	0.005	8.305

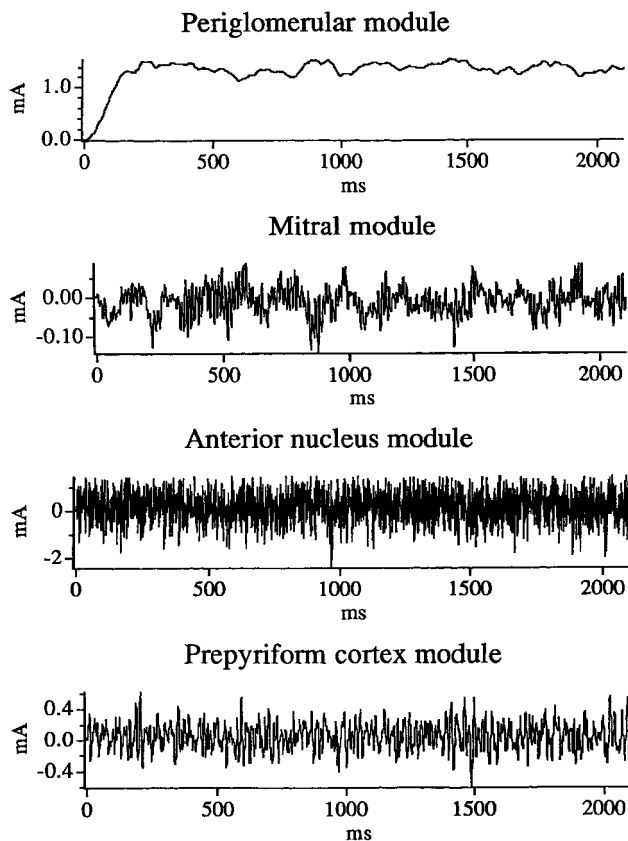


Fig. 3. Time series are from representative PG, OB, AON, PC nodes.

example in Fig. 3 shows the time series of representative KI_p , KI_{m1} , KI_{e1} , and KI_{a1} nodes, with the initial transit from an unstable fixed point to its stable performance under noise. The spectrum and amplitude histogram superimposed on its nonlinear gain, dp/dv , the derivative of its sigmoid, show that the distribution of the wave density values is wholly above the wave value, $v_{max} = \ln(Q_m)$, at peak gain for KI_p (Fig. 4), and wholly to the left of v_{max} for KI_{m1} (Fig. 5), KI_{e1} and KI_{a1} . During bursts the distributions of wave amplitudes for both the excitatory and inhibitory nodes in the OB, AON, and PC are wider but stay left of v_{max} .

IV. EVALUATION OF STABILITY

A. Stability with Fixed Parameters

Thus far the state of the KIII model was evaluated by visual inspection of the ensemble of time series, by which conformance to the established patterns of the EEG's could be judged. The need was recognized for numerical descriptors of the global state, that could be used to determine whether the model persisted in a designated initial state of arbitrary duration, and whether it returned to the same state reliably after repeated induction of gamma bursts. The test would characterize the present state of the KIII model automatically without requiring detailed inspection of the time series, and it would assign a probability value to the likelihood of return of the KIII model to the same attractor basin as before an induced state transition. A method was adapted from classification of

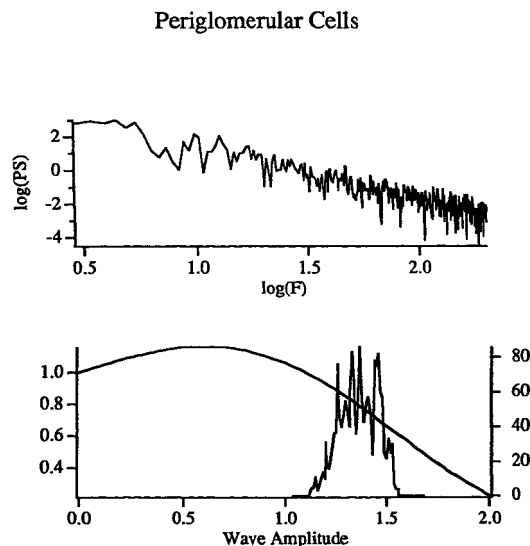


Fig. 4. The power spectrum and amplitude histogram are from a PG (KI_p) node.

EEG spatial patterns [1], [2], [29], by which the amplitude of the common wave form was taken from each of 64 simultaneously recorded traces, formed into a 64×1 column vector, and plotted as a point in 64 space. Recurrent patterns formed a normally distributed cloud of points with a center of gravity ("centroid") that defined the class of pattern by its spatial ensemble average. The radius of the cluster measured by the standard deviation (SD) defined the probability of

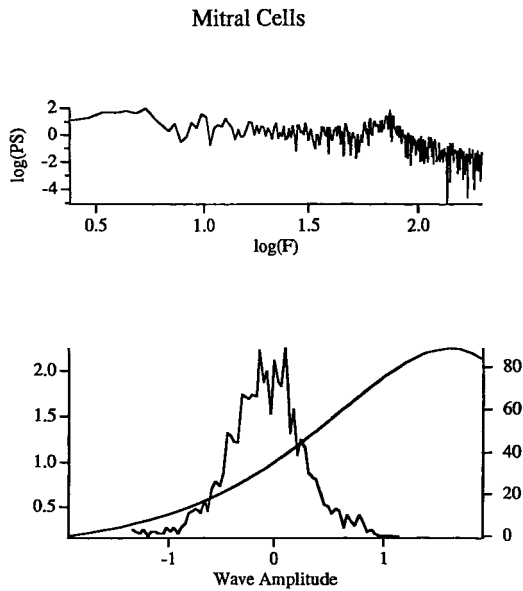


Fig. 5. The power spectrum and amplitude histogram are from the OB (KI_{m1} mitral cell) time series.

membership in the class. The distance of separation of two or more classes was evaluated by the distance between their centroids divided by the geometric mean of the two SD's.

For the KIII model a set of nine traces was taken from representative nodes (P , M_1 , M_2 , G_1 , E_1 , I_1 , A_1 , B_1 , and C). The traces were cut into 200 ms segments. Each segment gave seven measures (the four moments: mean, SD, skewness, and kurtosis; and the slope, intercept, and SD from the fitted $1/f$ line of the power spectrum in log-log coordinates, $9 \times 7 = 63$), plus the mean correlation by z -transform between pairs of KI_m subsets to evaluate the commonality of wave form. Evaluation of the distribution of points along each of the axes in 64-space combined with visual inspection of the traces showed that the skewness, kurtosis, and spectral estimates varied too greatly, so they were dropped. The g/d ratio was added [30], giving a point in 28-space ($9 \times 3 + 1$) for each measured time segment of the model.

A continuous run was initiated, and after the ~ 700 ms required for initialization of the model, a sample of ten segments of 200 ms at intervals of 1000 ms was evaluated to give a normally distributed cluster of 10 points with its centroid and SD. If the points showed no drift, and no points were more than 2 SD from the centroid, the system was judged to be stable. The value of the threshold SD was validated by visual inspection to confirm that the of all the time series in every segment conformed to the nine criteria listed. The test was repeated with durations up to 50 s, and then with 200 ms step segments given at 1 s intervals to induce gamma bursts. Test segments taken prior to the inputs showed that, despite the unpredictable variation in the wave forms of the multiple time series, the KIII system returned to the same basal state, within 200 ms after each input step segment was ended. The same result followed delivery of step inputs with varying amplitudes and spatial patterns, after input normalization and range compression in the manner described above.

B. Effects of Variation of Parameters

The set of 24 gains to be optimized was too large to be evaluated in one step. Each parameter was varied from its optimized value over a range sufficient to reveal instability in both directions, with the intent to rank the parameters in order of sensitivity, and then jointly to change those few simultaneously in accordance with optimization procedures already reported [12]. Each stepwise change in a parameter changed measurements in 28-space giving apparent drift of the centroid by its mean, SD, peak frequency, and amplitude distribution of the traces. A new criterion for instability was adopted. The time ensemble average A and SD were calculated for the set of statistics from the 10 segments (mean, SD, and g/d ratio), and they were plotted as a function of the parameter value. The new criterion that emerged was the SD of the cluster, which increased markedly between stable domains outside both ends of the range of acceptable function. The simulated neural activity patterns in those upper and lower flanking domains did not conform to experimental observations from the olfactory system. By this new criterion, each parameter tested was shown to have a substantial range in which the model was stable (Table I).

V. DISCUSSION AND CONCLUSIONS

The analysis and evaluation of the performance of the KIII model are still strongly dependent on visual inspection, so that further developments of stability assays are in progress. The criteria for conformance of the KIII model to EEG data are being expressed as fuzzy membership functions [30], either trapezoidal for average values (P -functions) or half-trapezoidal for variances (G -functions). Classification of the simulated EEG segment as acceptable or not are by the continued product (fuzzy AND operation) of the set of membership values. Membership functions are also being constructed for the stability criteria. A global stability rating on a graded scale is to be calculated from their continued product. Further options may be the use of weights to emphasize or attenuate subsets of criteria. The interactions of multiple parameters varied simultaneously are yet to be evaluated.

The robustness and stability of attractor states in the olfactory system are attested by its capacity to support the identification of familiar odors recurring over long periods of time, and by the reproducibility of the measurements of its spatiotemporal neural activity patterns. Its capacity to transit rapidly and repeatedly through its attractors underlies its service in olfactory pattern classification [31]. The global robustness of this highly unstable neural mechanism, in the face of continuing processes of growth, learning, and unlearning [32] must be maintained by chemical and neurohumoral controls exercised both locally and from the brain stem centrifugally, though little is known about them. At present the global stability of the KIII model is maintained and assayed by reference to criteria extracted by experimental studies, which appear to reflect system invariants that may or may not be used by the brain and the olfactory system, but are useful here.

Networks of nonlinear ODE's serve to simulate the olfactory EEG's and pulse densities when their parameters are adjusted to give aperiodic time series indicative of chaotic attractors. However, this approach brings three difficult problems. First, the sensitivity to initial conditions may be desirable for classification of very weak patterned inputs, but it opens a door nonselectively. Second, the aperiodic time series for successive real inputs are never identical, so the identification of an attractor for a recurring real input cannot be done by curve fitting. The problem is compounded in the high dimensional arrays of the KIII model with multiple uncorrelated time series. Third, in digital representations of the model the ODE's become difference equations. These are satisfactory for getting point and limit cycle solutions, but the truncation of the numbers in numerical approximations leads inevitably to numerical instabilities that may be difficult or impossible to distinguish from chaotic time series.

The solution for these problems by use of additive noise was suggested by analysis of the olfactory system, in which noise is always present from its receptors and its centrifugal controls. Endogenous noise is also present [27], both in additive form as a manifestation of action potentials, and in multiplicative form reflecting variation of neuronal parameters. However, neither the addition of random numbers to internal state variables, nor the random variation of parameters to give multiplicative noise, sufficed alone for stabilization, nor did they improve performance in the presence of the specified noise sources. It now appears that noise is not only unavoidable; it is also essential. This means that the attractor states manifested both in the model and in the olfactory system are not chaotic. They are hybrid. Chaotic attractors, like straight lines and perfect spheres, do not exist in nature, but are mathematical fictions to help in system design. The question, "Is brain activity chaos or colored noise?" is answered, "neither," by this hypothesis. The ratio of amplitudes by which they coexist can be calculated in models, as in the present case, but whether the simulations are accurate for the biological systems has not been determined.

Future testing of this hypothesis may be done in analog computation, in which numerical instabilities are not at issue. Earlier attempts to develop analog embodiments [33], [34] were abandoned owing to component imprecision, drift with temperature and aging, and especially the $1/f$ -type noise in the operational amplifiers, which foretold that emergence of the desired property in KIII outputs could not be distinguished from capture of the global system by any one of its numerous elements. The present finding indicates that an analog approach should be re-explored to determine whether the intrinsic noise of components, particularly when they are reduced in size for LSI and VLSI, can be used to simulate action potentials in place of random number generators. Such an approach may solve another major problem, which is the amount of computational resource that is required for digital solution of ODE's. It is unlikely that models deriving from chaotic neurodynamics can be brought into the commercial and industrial arenas, until they are embodied in fully parallel analog or hybrid digital-analog devices. The taming of chaos by noise may open a path to that development.

Particular note should be taken that the use of noise that is shown in this paper does not serve either to induce or suppress chaotic attractors, as described by others [34]–[37], but to maintain existing or desired chaotic attractors.

REFERENCES

- [1] J. M. Barrie, W. J. Freeman, and M. Lenhart, "Modulation by discriminative training of spatial patterns of gamma EEG amplitude and phase in neocortex of rabbits," *J. Neurophysiol.*, vol. 76, pp. 520–539, 1996.
- [2] W. J. Freeman and K. A. Grajski, "Relation of olfactory EEG to behavior: Factor analysis," *Behav. Neurosci.*, vol. 101, pp. 766–777, 1987.
- [3] L. M. Kay, K. Shimoide, and W. J. Freeman, "Comparison of EEG time series from rat olfactory system with model composed of nonlinear coupled oscillators," *Int. J. Bifurc. Chaos*, vol. 5, pp. 849–858, 1995.
- [4] W. J. Freeman, "Tutorial in Neurobiology: From single neurons to brain chaos," *Int. J. Bifurc. Chaos*, vol. 2, pp. 451–482, 1992.
- [5] Y. Yao, W. J. Freeman, B. Burke, and Q. Yang, "Pattern recognition by a distributed neural network: An industrial application," *Neural Networks*, vol. 4, pp. 103–121, 1991.
- [6] K. Shimoide and W. J. Freeman, "Dynamic neural network derived from the olfactory system with examples of applications," *IEICE Trans. Fundament.*, vol. E-78A, pp. 869–884, 1995.
- [7] W. J. Freeman, *Mass Action in the Nervous System*. New York: Academic, 1975.
- [8] ———, "Simulation of chaotic EEG patterns with a dynamic model of the olfactory system," *Biolog. Cybern.*, vol. 56, pp. 139–150, 1987.
- [9] ———, "Strange attractors govern mammalian brain dynamics, shown by trajectories of electroencephalographic (EEG) potential," *IEEE Trans. Circuits Syst.*, vol. 35, pp. 781–783, 1988.
- [10] Y. Yao and W. J. Freeman, "Model of biological pattern recognition with spatially chaotic dynamics," *Neural Networks*, vol. 3, pp. 153–170, 1990.
- [11] W. J. Freeman and S. Jakubith, "Bifurcation analysis of continuous time dynamics of oscillatory neural networks," in *Brain Theory. Spatio-temporal Aspects of Brain Function*, A. Aertsen and W. von Seelen, Eds. Amsterdam: Elsevier, 1993, pp. 183–208.
- [12] H.-J. Chang and W. J. Freeman, "Parameter optimization in models of the olfactory system," *Neural Networks*, vol. 9, pp. 1–14, 1996.
- [13] W. J. Freeman, "Random activity at the microscopic neural level in cortex ("noise") sustains and is regulated by low-dimensional dynamics of macroscopic cortical activity ("chaos")," *Int. J. Neural Syst.*, vol. 7, pp. 473–480, 1996.
- [14] K. Wiesenfeld and P. Hadley, "Attractor crowding in oscillator arrays," *Phys. Rev. Lett.*, vol. 62, pp. 1335–1338, 1989.
- [15] K. Y. Tsang and K. Wiesenfeld, "Attractor crowding in Josephson junction arrays," *Appl. Phys. Lett.*, vol. 56, pp. 495–496, 1990.
- [16] W. J. Freeman, H.-J. Chang, and B. C. Burke, "Limitations on numerical simulations of chaotic dynamics observed in brain systems," in *Proc. Int. Symp. Nonlinear Theory and It Applicat. I*, 1995, pp. 10–14.
- [17] W. L. Ditto, S. N. Raueo, and M. L. Spano, "Experimental control of chaos," *Phys. Rev. Lett.*, vol. 26, pp. 3211–3214, 1990.
- [18] L. M. Pecora and T. L. Carroll, "Pseudoperiodic drifting: Eliminating multipole domains of attraction using chaos," *Phys. Rev. Lett.* vol. 67, pp. 945–948, 1991.
- [19] T. L. Carroll and L. M. Pecora, "Stochastic resonance and chaos," *Phys. Rev. Lett.*, vol. 70, pp. 576–579, 1993.
- [20] H. Liljenström and X.-B. Wu, "Noise-enhanced performance in a cortical associative memory model," *Int. J. Neural Syst.*, vol. 6, pp. 19–29, 1995.
- [21] K. Y. R. Billah and M. Shinozuka, "Stabilization of a nonlinear system by multiplicative noise," *Phys. Rev. A*, vol. 44, pp. 4779–4781, 1996.
- [22] R. Wackerbauer, "Noise-induced stabilization of the Lorenz system," *Phys. Rev.*, vol. 52, pp. 1335–1338, 1995.
- [23] S. T. Fryska and M. A. Zohdy, "Computer dynamics and shadowing of chaotic orbits," *Phys. Lett. A*, vol. 166, pp. 340–346, 1992.
- [24] S. M. Hammel, J. A. Yorke, and C. Grebogy, "Do numerical orbits of chaotic dynamical processes represent true orbits?" *J. Complexity*, vol. 3, pp. 136–145, 1987.

- [25] C. Grebogyi, S. M. Hammel, J. A. Yorke, and T. Sauer, "Shadowing of physical trajectories in chaotic dynamics: Containment and refinement," *Phys. Rev. Lett.*, vol. 65, pp. 1527–1530, 1990.
- [26] S. Dawson, C. Grebogyi, T. Sauer, and J. A. Yorke, "Obstructions to shadowing when a Lyapunov exponent fluctuates about zero," *Phys. Rev. Lett.*, vol. 73, pp. 1927–1930, 1994.
- [27] W. J. Freeman, "Random activity at the microscopic neural level in cortex ('noise') sustains and is regulated by low-dimensional dynamics of macroscopic cortical activity ('chaos')," *Int. J. Neural Systems*, vol. 7, pp. 473–480, 1996.
- [28] M. Zak, "Terminal chaos for information processing in neurodynamics," *Biol. Cybern.*, vol. 64, pp. 343–351, 1991.
- [29] W. J. Freeman, "Techniques used in the search for the physiological basis of the EEG," in *Handbook of Electroencephalography and Clinical Neurophysiology*, A. Gevins and A. Remond, Eds. Amsterdam: Elsevier, 1987, vol. 3A, ch. 18, pp. 583–664.
- [30] J. Badler, "A fuzzy logic algorithm for determining stability limits of KIII system parameters," to be posted on the Home Page of the Freeman Laboratory: <http://sulcus.berkeley.edu>, 1997.
- [31] C. A. Skarda and W. J. Freeman, "How brains make chaos in order to make sense of the world," *Behav. Brain Sci.*, vol. 10, pp. 161–195, 1987.
- [32] W. J. Freeman, "Societies of brains," in *A Study in the Neuroscience of Love and Hate*. Hillsdale, NJ: Lawrence Erlbaum, 1995.
- [33] ———, "Analog simulation of prepyriform cortex in the cat," *Math. BioSci.*, vol. 2, pp. 181–190, 1968.
- [34] J. Eisenberg, W. J. Freeman, and B. Burke, "Hardware architecture of a neural network model simulating pattern recognition by the olfactory bulb," *Neural Networks*, vol. 2, pp. 315–325, 1989.
- [35] H. Herzog, "Stabilization of chaotic orbits by random noise," *Zeitschrift angewandte Mechanik*, vol. 11, pp. 582–583, 1988.
- [36] K. Matsumoto and I. Tsuda, "Noise-induced order," *J. Statist. Phys.*, vol. 31, pp. 87–106, 1983.
- [37] T. Kapitaniak, *Chaos in Systems with Noise*. Singapore: World Scientific, 1988.
- Walter J. Freeman** studied electronics, physics, and mathematics at the Massachusetts Institute of Technology, Cambridge, and literature and philosophy at the University of Chicago, Chicago, IL. He received the medical degree (cum laude) from Yale University, New Haven, CT, in 1954, and began post-Doctoral training in pathology and internal medicine at Johns Hopkins University, Baltimore, MD, and neurobiology at the University of California, Los Angeles, as Fellow of the Foundations Fund for Research in Psychiatry. Since 1959, he has taught physiology at the University of California, Berkeley. His research interests lie in mathematics modeling of nonlinear neurodynamics, based on his experimental measurements of brain activity in behaving animals, and the application of these models in biology, neurology, psychiatry, philosophy, and industry. Dr. Freeman received the A. E. Bennett Award of the Society of Biological Psychiatry (1964), Guggenheim Award (1966), Titulaire de la Chaire Solvay, University of Brussels (1974), the MERIT Award from NIMH (1990), the Pioneer Award from the Neural Network Council of the IEEE (1991), and the Spinoza Chair of the University of Amsterdam (1995). In 1994, he was President of the International Neural Network Society.
- H.-J. Chang**, photograph and biography not available at the time of publication.
- B. C. Burke**, photograph and biography not available at the time of publication.
- P. A. Rose**, photograph and biography not available at the time of publication.
- J. Badler**, photograph and biography not available at the time of publication.